EFFECTS OF OROGRAPHIC GRAVITY WAVE DRAG IN THE MARTIAN ATMOSPHERE BY PARAMETERIZATION AND GRAVITY WAVE-RESOLVING SIMULATIONS

A. Kling , *NASA Ames/BAERI (alexandre.m.kling@nasa.gov)*, **R. J Wilson, A. Brecht**, **M. Kahre**, *NASA Ames*, **J. Murphy**, *NMSU, New Mexico, USA*

Introduction:

Gravity or inertia-gravity waves are ubiquitous in the Martian atmosphere [1, 2]. Gravity waves (GWs) are described as orographic when they are excited by an isentropic displacement of low-level winds that encounter an obstacle (topography) or non-orographic when the source of the perturbation is dynamic (e.g., convection, jet/front systems). In the mesosphere and in the thermosphere, GWs may break and interact with planetary waves, triggering secondary waves [3, 4, 5] and dynamically alter the circulation and thermal structure.

In principle, the effects of GWs could be incorporated into Mars Global Climate Models (MGCMs) by explicitly resolving them and validating the results against extant observations, as can be done with Mars's baroclinic waves and thermal tides. In that respect, some numerical studies have involved explicitly-resolved GWs with mesoscale local-area simulations [6, 7], and "high-resolution" global modeling [8]. Because of their non-linear nature, short vertical wavelength and small horizontal scale (few 10s-100s of km) GWs have remained challenging to resolve explicitly on a global scale. It is therefore generally more practical to parameterize GWs as sub-grid scale processes using either orographic [9, 10] or non-orographic [11, 12, 13] numerical schemes. In this study, we bridge the two methods used to represent GWs in MGCMs by comparing the parameterized and explicitly-resolving approaches against each other, focusing at first on the orographic waves since the source of these waves (displacement of air flow over topographic surfaces) is most readily understood.

Simulation set-up:

Orographic gravity wave drag scheme. The orographic scheme from Palmer et al. (1986) [14] is used for the treatment of unresolved mountain waves, and we summarize here the basics of its implementation. The variance of the unresolved orography to the mean elevation is multiplied by the low level winds (among other terms) to obtain the surface base flux for the gravity wave. Working upward through the atmospheric column, the stability of the layers compared to the gravity wave is evaluated. When saturation is detected (wave breaking occurs), momentum is transferred to the atmosphere in the form of a deceleration tendency (drag in [m/s/sol]) that is applied to both the zonal and meridional winds. The implementation includes the wavelength-dependent thermal damping rates from [15].

Grid set-up and mesosphere-specific physics. For this study, we tested a set of varying horizontal resolutions ranging from ~3.75° to 0.25° and constant vertical resolutions in the mesosphere ranging from 3 km to 800 m (60-520 layers). Hereafter we refer to "Gravity-Wave Resolving Simulations" (GWRS) as any simulation of horizontal resolution $\leq 1°$ and vertical resolution < 3 km in the mesosphere, and therefore suitable for resolving some of the GWs' spectrum. For reference, a baseline grid set-up for the MGCM would typically use ~3.75° of horizontal resolution and vertical layers of increasing thicknesses, with a top layer on the order of 10 km thickness at ~100 km. The CO_2 15 μm cooling parameterization is adapted from [16] and dependent on temperature, CO_2 density, and atomic oxygen density which are self-consistently computed. The simulations do not include UV-heating and molecular diffusion, so while we place the model top at ~150 km to mitigate wave reflection, we only focus on the 0-120 km domain for our analysis.

Treatment of aerosols. In the MGCM, the microphysics is sensitive to the physical time step, which is in turn connected to the dynamical timestep and therefore adjusted as the horizontal and vertical resolutions change. In order to isolate the effects of varying spatial resolution on the dynamics from radiative effects due to aerosols, we use a simple prescription for the aerosols that do not include water-ice or CO_2 microphysics, nor their respective radiative forcings. For the dust, we use the analytically prescribed 'MGS' scenario that is independent of the resolution [17].

Evidence for GWs activity at refined horizontal and vertical resolutions:

We show here qualitative examples of resolved GW activity. Figure 1 shows daytime vertical winds at 80 km (shaded colors) above the Tharsis plateau from a 0.25°/90 layers simulation at L_s 110°. Concentric waves are localized above Olympus Mons

and the Tharsis volcanoes, demonstrating that orographic waves are explicitly resolved and propagate well into the mesosphere.

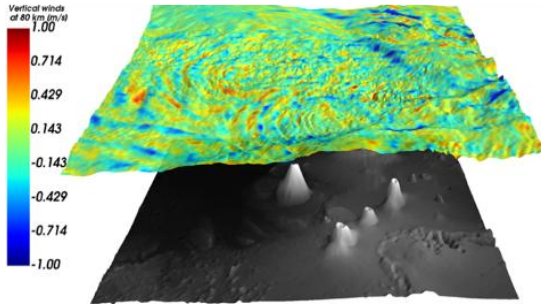

Figure 1: Vertical winds at 80 km altitude show concentric orographic waves in the Tharsis region.

In Figure 2, we apply a standard technique to retrieve wave features from the global outputs of the GWRS: Temperature variances are retrieved from the model outputs by subtracting an individual temperature profile to its low-order polynomial fit. The detrended perturbations on the native pressure layers are re-sampled on a uniform grid and a Fourier analysis using the Welch method is used to extract vertical wavenumbers and associated power spectral densities (PSD). Finally, resulting PSDs from individual profiles are binned by region and altitudes of interest (lower half of the mesosphere 0-50 km and upper half 50-100 km). This procedure has been used in observational studies for GW retrieval (e.g. radio-occultation [18, 19]) which offer opportunities for model validation. Several features are accurately captured by the GWRS. First, we note that the slope of the PSD decreases with increasing vertical wavenumber (decreasing wavelength), which is consistent with waves of shorter wavelengths being dissipated. Second, we note that the PSD for waves in the upper mesosphere (solid lines) are one order of magnitude higher than in the lower mesosphere (dashed lines), which is consistent with the growth in amplitude of orographic and non-orographic GWs as they propagate upward.

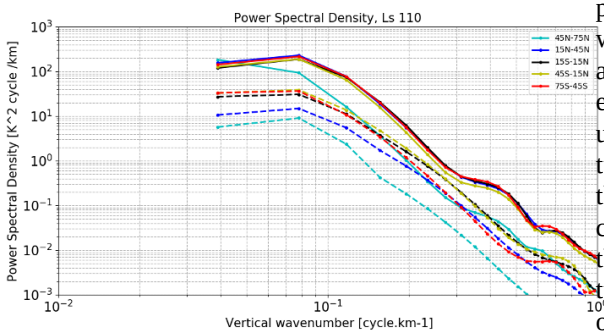

Figure 2: Vertical wave spectrum as observed from GWRS.

Nature of the dominant gravity waves during the southern winter:

In Figure 3, we show the zonally-averaged temperature and winds at L_s 90° for a simulation at 3.75° horizontal resolution and without the GW-drag parameterization. This simulation is used as our baseline case. MGCM simulations at this season are known to be susceptible to a cold bias in southern polar temperatures. [9]

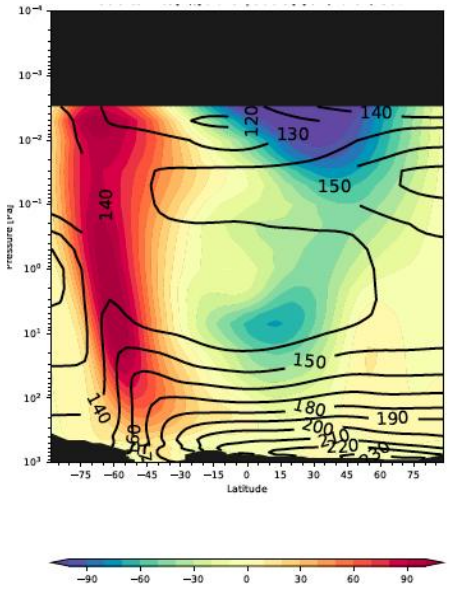

Figure 3 Reference zonal winds (shaded contours) and temperature (solid contours) from the reference 3.75° simulation at L_s 90°.

We computed the range for phase speeds of gravity waves originating from the surface at this season (either of orographic source or other dynamic processes localized immediately near the ground) and organized those into different latitude bins. This calculation tests for filtering of gravity waves harmonics by the mean winds as they propagate upward and shows the range of allowed phase speeds at any given height. Given that orographic waves have low phase speeds (the source for the waves is the orography and therefore static), this calculation highlights what type of waves may be expected throughout the atmosphere. In Figure 4, it is seen that in the southern latitudes (bottom three graphs in the first column), low phase speeds are able propagate to altitudes 80-100 km whereas at the equator (top graph in the first column) or in the northern latitudes (second column), low phase speeds are filtered well before they reach any significant altitude. Orographic gravity waves are therefore expected to have an impact only in the southern hemisphere at this season.

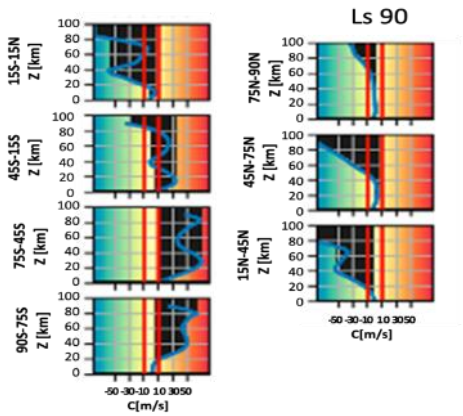

Figure 4: Allowed phase speeds as a function of height at L_s 90° for different latitude bins. Black shades show forbidden domain and white shades show low phase speeds. The red vertical lines show the +/- 10 m/s domain as a reference.

Comparison of resolved and parameterized GW drag:

The Palmer (1986) parameterization implemented in the MGCM uses a coupling factor as a tuning parameter, effectively controlling the surface base flux. Since a main application of GW drag schemes is to alleviate biases in atmospheric temperature due to unresolved waves, one approach is to tune the schemes against available temperature observations (e.g., Mars Climate Sounder). This is an indirect approach in the sense that the output of the scheme (a GWs-induced deceleration tendency in [m/s/sol]) is adjusted based on its dynamical effects on the overall temperature structure. It therefore requires aerosols forcings and other physics to be well-enough represented in the MGCM simulation to be consistent with the reference observations. GWRS offer an additional, and more direct, comparison point as the resolved zonal wave-mean flow forcing $ax = 1/\rho \, d(\rho \, u'w')/dz$ [m/s/sol] can be directly compared against the output from the parameterization.

In Figure 5, we compare the GW drag and its effect on the temperature structure for a 3.75° simulation with GW drag parameterization (top row) and for a 0.25° GWRS with no parameterization. Both cases are compared against the reference simulation (3.75° with no GW parameterization, as shown in Figure 3).

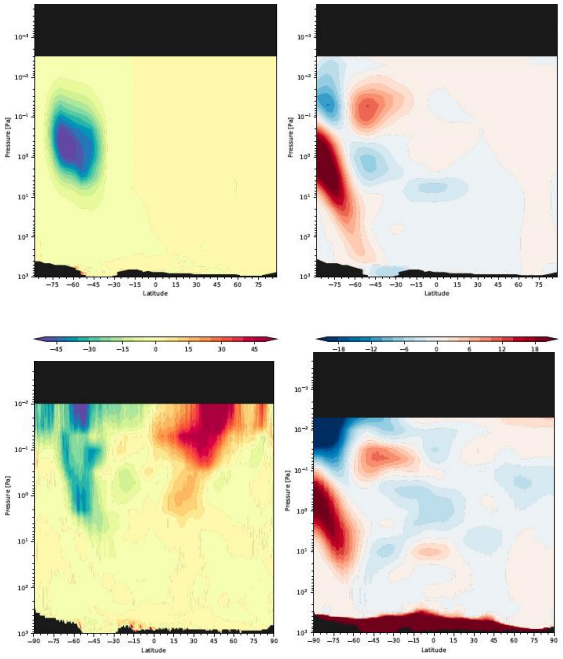

Figure 5: GW forcings in [m/s/sol] (left column), and temperature difference (right column) against the baseline simulation with no GW parameterization. Top row is with the parameterization and bottom row is with the GWRS.

Figure 5 shows good agreement between the wave-mean flow forcings produced by the parameterization and those calculated from the GWRS in the southern hemisphere at the 1-0.1 Pa level. The forcing has a negative sign implying that the effect is to decelerate the circulation. In the northern hemisphere, the GWRS shows positive forcing (acceleration) which is not present with the GW parameterization, implying the mechanism at play is not orographic in nature. The dynamical effects for both the parameterization and the GWRS are consistent and on the order of +20 K warming at the 1Pa level for the southern pole. Adjacent cooling in the column at the 0.01 Pa level and warming in the order of +5 K at the 0.1 Pa level in the southern tropics are also consistent between the GWRS and the parameterization. The GWRS shows additional forcings near the top of the model which is not present in the parameterization. This indicates that a much richer spectrum of waves is represented in the GWRS than can be accounted for in the parameterization, which is based on a single wavelength.

Effect of orographic GWS drag on the climatology:

The agreement in the amplitudes for the wave-mean flow forcings and the resulting dynamical effects on the temperature structure between the GWRS and the parameterization suggests that the

parameterization is performing as intended. It is therefore a convenient way to investigate the season and location where orographic GW are prominent.

The calculation of allowed phase speed at L_s 270° (not shown) suggests that the northern winter is the other main season when orographic gravity waves are allowed to propagate to the upper mesosphere. Figure 6 shows the GW forcings resulting from the tuned parameterization at the 0.1 Pa level for an annual cycle. GW drag (as a decelerating effect) is prominent at L_s 30-170° in the southern latitudes (50 S to 75 S) and in the northern latitudes (80 N) at L_s 200-300°.

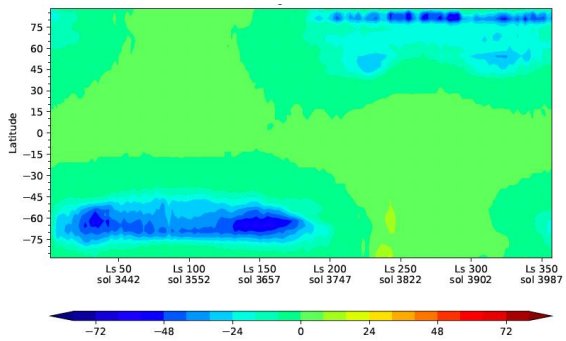

Figure 6: Wave mean flow forcings [m/s/sol] at the 0.1 Pa level from the orographic GW drag parameterization.

It was found that the surface base flux for the orographic GWs does not show a strong correlation with the observed drag at higher altitude (e.g., at 0.1 Pa in Figure 6). This explains why GWs forcing by orographic waves is also observed during the northern winter, while the northern plains are comparatively mostly absent of orography: suitable conditions allowing for the upward propagation of GWs are more important to wave growth than the amplitude of the initial perturbation.

Conclusions:

GWRSs at sub-degree (1/4°) horizontal resolution with fine vertical structure (~100 layers) provide a direct method to tune and validate subgrid-scale parameterizations of wave-mean flow forcings due to unresolved GWs. In this study, the resulting effect of GWs on the temperature structure, namely a +20 K dynamical warming of the southern pole at the ~1Pa level is attributed to orographic gravity waves and is remarkably consistent between the two methods at L_s 90°. GWRS are a promising method to fill observational gaps in the GW climatology as they offer a comparison point to GW observations, such as radio-occultations [18] or remote sensing observations [2]. We foresee GWRSs as being insightful for the tuning of non-orographic GWS subgrid-scale parameterizations, for those little is known about the sources of those waves.

References:

[1] Vals et al. (2019) *Planetary and Space Science* 178 [2] Heavens et al. (2020) *Icarus, 113630* [3] Williams et al. (1999) *Advances in Space Research 24* [4] Fritts and Alexander (2003) *Reviews of Geophysics 41* [5] Kshevetskii and Gavrilov (2005) *Journal of Atmospheric and Solar- Terrestrial Physics 67* [6] Spiga, et al. (2012) *Geophysical Research Letters 39* [7] Imamura et al. (2016*) Icarus 267* [8] Kuroda et al. (2020) *JGR Planets 125* [9] Forget et al. (1999) *JGR Planets 104* [10] Collins et al. (1997) *Advances in Space Research 19* [11] Medvedev et al. (2015) *JGR Planets* 120 [12] Yiğit et al. (2018) *Annales Geophysicae 36* [13] Gilli et al. (2020) *JGR Planet 125* [14] Palmer et al. (1986) *Quarterly Journal of the Royal Meteorological Society* 112 [15] Eckermann et al. (2011) *Icarus 211* [16] Bougher et al. (2006) *Geophysical Research Letters 33* [17] Montmessin et al. (2004) *J. Geophys. Res.*, 109 [18] Ando et al. (2012) *Journal of the Atmospheric Sciences* 69 [19] Tellmann et al. (2013) *JGR Planets 118*